GEOPHYSICS, VOL. 68, NO. 1 (JANUARY-FEBRUARY 2003); P. 210–224, 8 FIGS., 2 TABLES.
10.1190/1.1543208

Traveltime and conversion-point computations and parameter estimation in layered, anisotropic media by τ-p transform

Mirko van der Baan* and J.-Michael Kendall*

ABSTRACT

Anisotropy influences many aspects of seismic wave propagation and, therefore, has implications for conventional processing schemes. It also holds information about the nature of the medium. To estimate anisotropy, we need both forward modeling and inversion tools. Forward modeling in anisotropic media is generally done by ray tracing. We present a new and fast method using the τ-p transform to calculate exact reflection-moveout curves in stratified, laterally homogeneous, anisotropic media for all pure-mode and converted phases which requires no conventional ray tracing. Moreover, we obtain the common conversion points for both P-SV and P-SH converted waves. Results are exact for arbitrary strength of anisotropy in both HTI and VTI media (transverse isotropy with a horizontal or vertical symmetry axis, respectively).

Since inversion for anisotropic parameters is a highly nonunique problem, we also develop expressions describing the phase velocities that require only a reduced number of parameters for both types of anisotropy. Nevertheless, resulting predictions for traveltimes and conversion points are generally more accurate than those obtained using the conventional Taylor-series expansions. In addition, the reduced-parameter expressions are also able to handle kinks or cusps in the SV traveltime curves for either VTI or HTI symmetry.

INTRODUCTION AND MOTIVATION

In anisotropic media, many wave phenomena occur which are counterintuitive to our conception of isotropic wave motion. To account for these effects, successful data processing requires a high level of knowledge concerning the way particular anisotropy parameters affect the data. To a certain extent, insights can be gained through analytical treatments and forward modeling tools (e.g., by means of ray tracing). However, ultimately we need to assess the actual anisotropy parameters in a certain region. We therefore require accurate inversion tools. Furthermore, given the ever increasing size of data volumes, any modeling and inversion tools should be both fast and easy to implement.

In this paper, we extend the results of Van der Baan and Kendall (2002; hereafter, paper I), who demonstrated how the τ-p transform can be used both as a forward modeling tool to compute exact moveout curves of pure-mode data (e.g., P-P reflections) and as an inversion tool to extract the anisotropy parameters in transversely isotropic media with a vertical symmetry axis (VTI). We extend these results to also incorporate transversely isotropic media with a horizontal symmetry axis (HTI) and converted waves (e.g., P-SV reflections). In addition, this method can be used to calculate exact common conversion points in both symmetries for all offsets and azimuths. Finally, approximate solutions for the conversion points using a reduced set of parameters are also determined which are more suitable for inversion.

Conventionally, within the limit of ray theory, exact traveltimes and conversion points are calculated by means of ray-tracing methods (Gajewski and Pšenčík, 1987; Kendall and Thomson, 1989). Unfortunately, their implementation is rather involved, even for simple laterally homogeneous media. Furthermore, their extension to a complete anisotropic tomography approach in 3D is also rather prohibitive [see, for instance, Chapman and Pratt (1992) for a 2D approach].

Another method for solving the forward problem is to use Taylor-series expansions (Tsvankin and Thomsen, 1994; Alkhalifah and Tsvankin, 1995; Al-Dajani and Tsvankin, 1998; Thomsen, 1999). However, this does not yield exact results, and their applicability is currently limited to VTI media for converted-wave phases (Tsvankin and Thomsen, 1994). For pure-mode data, expressions for orthorhombic media exist (Al-Dajani et al., 1998; Al-Dajani and Toksöz, 1999). In paper I, we demonstrated that the traveltime predictions of the τ-p method using reduced-parameter

Published on Geophysics Online July 19, 2002, Manuscript received by the Editor August 22, 2001; revised manuscript received May 24, 2002.
*University of Leeds, School of Earth Sciences, Woodhouse Lane, Leeds LS2 9JT, United Kingdom. E-mail: mvdbaan@earth.leeds.ac.uk; kendall@earth.leeds.ac.uk.

expressions are more accurate than those of the conventional Taylor-series approach for VTI media. In this paper, we show that this is even more true for the predictions of the conversion points of P-SV converted waves in VTI media. Furthermore, contrary to the Taylor-series approach, our method is easily extended to also handle converted-wave traveltimes and common conversion points in, for instance, HTI media.

As an introduction, we illustrate the effects of anisotropy on traveltimes and conversion points using a simple model comprised of two layers over a half space. The upper layer is 500-m thick, isotropic, and has $\alpha_0 = 1.8$ km/s and $\beta_0 = 1.0$ km/s for the P- and S-wave velocities, respectively. The second layer is also 500 m thick and has isotropic background velocities of $\alpha_0 = 2.5$ km/s and $\beta_0 = 1.4$ km/s. Four models of anisotropy in the second layer are considered: (1) isotropy, (2) VTI anisotropy with Thomsen (1986) parameters ϵ, γ, $\delta = 0.05$ (elliptic anisotropy), (3) fluid (water)-filled fractures, and (4) gas-filled fractures. The fractures are vertically aligned (HTI media) with the normal to the crack face oriented in the offset direction. The crack density is 0.1, the crack aspect ratio is 0.001, and the theory of Hudson (1981) is used to construct effective-medium models. The traveltimes and raypaths in these media have been computed using the exact ray tracer ATRAK (Guest and Kendall, 1993). Figure 1 shows the slowness and wave surfaces for the four cases. Note that the P-wave velocity surfaces show a 180° periodicity in the gas-filled case and a 90° periodicity in the fluid-filled case.

Figure 2 shows the traveltimes for the four cases. For both the isotropic and the elliptic VTI model, any deviation from hyperbolic moveout in the P-wave traveltime curve is solely due to the effect of the overburden. The VTI model (long dashes) shows smaller traveltimes than the isotropic model (solid line), whereas the fracture cases show larger traveltimes. The largest differences are observed for the case of gas-filled fractures (dotted line), where traveltimes are late, even at short offsets. There is a clear difference between the fluid-filled (short dashes) and gas-filled (dots) fracture cases.

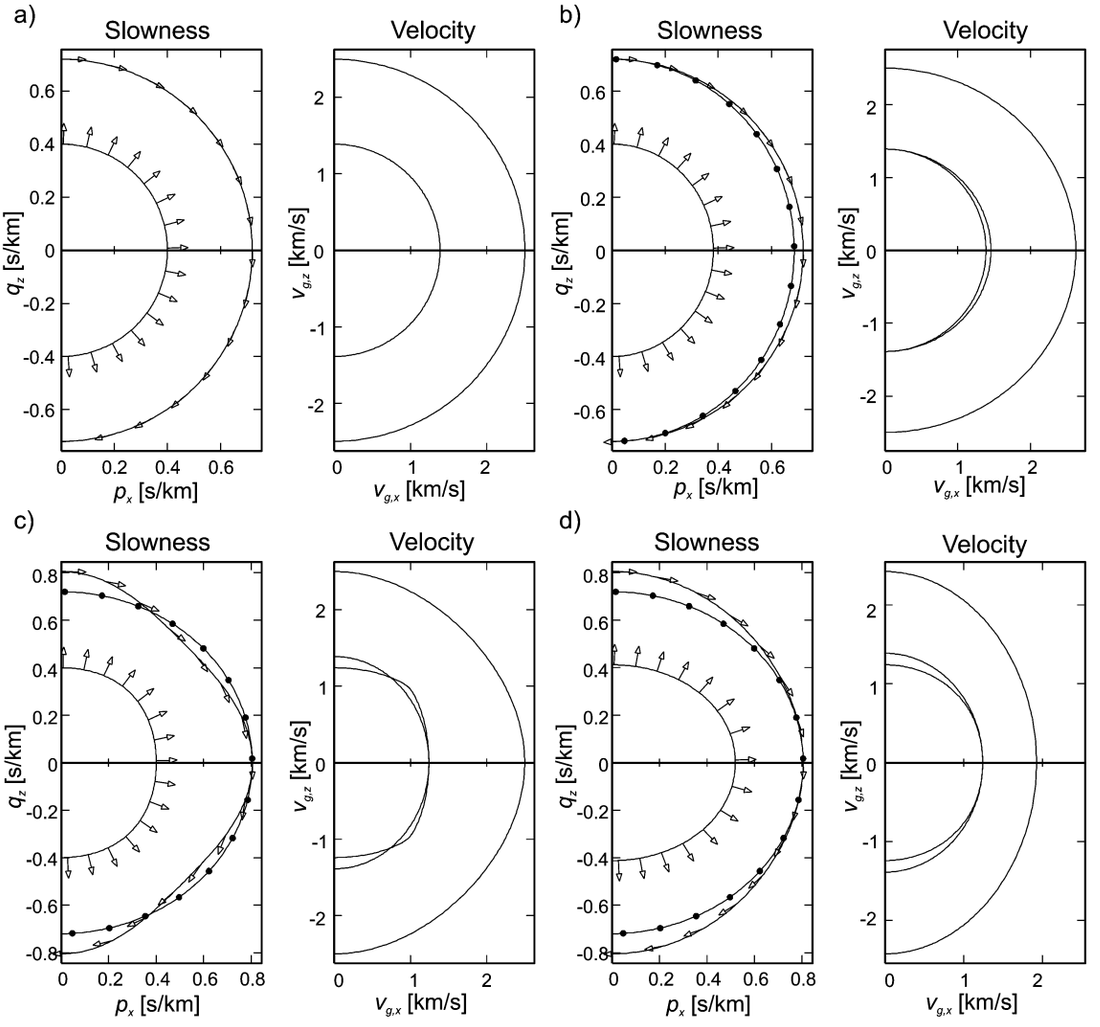

FIG. 1. Vertical slices of the slowness surfaces (left side) and wave surfaces (right side) for the second layer in four models. The particle motion for each wavesheet is indicated by vectors on the slowness surfaces. (a) Isotropic model, (b) transversely isotropic with a vertical symmetry axis (VTI), (c) vertically aligned fluid-filled fractures, (d) vertically aligned gas-filled fractures. The fracture density is 0.1, the aspect ratio is 0.001, and the normal to fracture plane is in the offset direction x. The anisotropic models display rotational symmetry around, respectively, the vertical (b) and horizontal axis [(c) and (d)].

Large differences occur in the converted-wave raypaths and therefore the conversion-point distributions. Figure 3 shows raypaths for P-wave reflections from the base of layer 2 at offsets of 200 and 900 m, and the associated P-SV converted waves. The four cases show large variations in converted-wave raypaths for constant P-wave emergence offset. In the fracture cases, there is little variation between the P- and SV-wave raypaths through the anisotropic layer which leads to converted-wave offsets which are very near the P-wave emergence offsets. Although the wavefront normals (i.e., the plane-wave propagation directions) are very different for the P- and SV-waves, the group velocities and therefore the raypaths are nearly aligned, especially in the fluid-filled fracture case. The large differences in converted-wave emergence offsets suggest that the actual location of the conversion point is very sensitive to the underlying cause of anisotropy. Therefore, accurately assessing the anisotropy parameters in a particular area is very important before data can be successfully sorted into common-conversion-point gathers.

In this paper, we first review the equations describing the form of the $\tau(\mathbf{p_r})$ curves. Next, we develop the required expressions for the phase velocities as a function of horizontal slowness in both HTI and VTI media, and we show how exact traveltime curves and conversion points can be computed in laterally homogeneous, layered media. We then derive reduced-parameter expressions which can be used in inversions for anisotropy parameters. Finally, a general inversion strategy is put forward, and we conclude with a numerical example using the elastic coefficients of a strongly anisotropic shale.

THEORY

Traveltimes and the slant stack

For an anisotropic earth composed of a stack of horizontal layers, Hake (1986) showed that there exists a direct link between the τ-p transform and the traveltime curves of reflections. Namely, the traveltime $t(x, y)$ can be linearly decomposed into

$$t = p_x x + p_y y + \sum_i z_i(\hat{q}_{z,i} + \acute{q}_{z,i}) = p_x x + p_y y + \tau, \quad (1)$$

where p_x and p_y represent the horizontal slowness in the x- and y-directions, respectively; z_i the thickness of layer i; $\hat{q}_{z,i}$ and $\acute{q}_{z,i}$ the absolute vertical slowness of, respectively, the down- and upgoing plane waves in that layer; and τ the total intercept time.

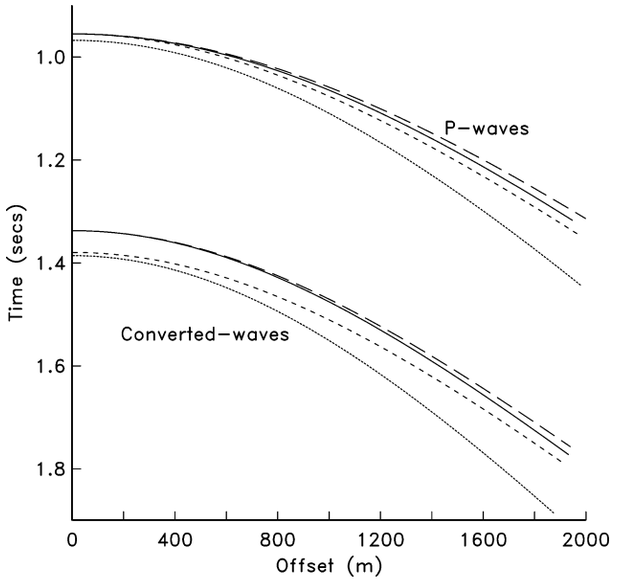

FIG. 2. Traveltimes for the four models: isotropic model (solid line), (elliptic) VTI model (long dashes), fluid-filled fractures (short dashes) and gas-filled fractures (dotted line).

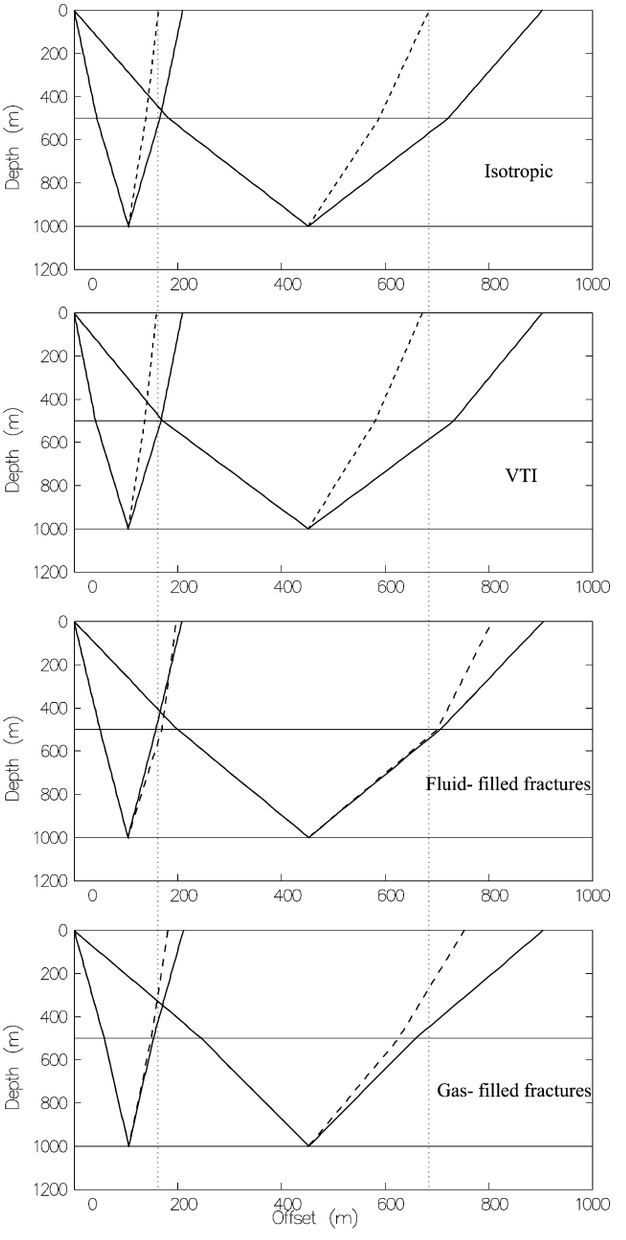

FIG. 3. Raypaths for P-waves (solid lines) and SV-waves (dashed lines) in the four models. From top to bottom, the properties of the second layer are: isotropic, elliptic VTI symmetry, fluid-filled fractures, gas-filled fractures.

Snell's law, which states that the horizontal slowness components p_x and p_y remain constant for horizontal layering, has been used to derive this exact equation. The τ-p transform can be identified in equation (1) since $z_i\grave{q}_{z,i}$ equals $\Delta\grave{\tau}_i$, the one-way intercept time of the downgoing plane wave in layer i for a given slowness, and the two-way intercept times $\Delta\tau_i$ add up linearly. That is,

$$\sum_i z_i(\grave{q}_{z,i}+\acute{q}_{z,i})=\sum_i(\Delta\grave{\tau}_i+\Delta\acute{\tau}_i)=\sum_i\Delta\tau_i=\tau. \quad (2)$$

Hake's (1986) result was originally formulated for a 2D medium. However, Diebold (1987) showed for the isotropic case that the relation between the traveltimes and the τ-p transform can be extended to three dimensions. This remains true for 3D anisotropic media.

To simplify the mathematical notation, we introduce the radial slowness in the horizontal plane $\mathbf{p_r}=(p_x, p_y, 0)^t$ with magnitude $|\mathbf{p_r}|=p_r$, and the emergence offset $\mathbf{r}=(x, y, 0)^t$ at distance $|\mathbf{r}|=r$ from the source. Hence, equation (1) simplifies to

$$t=\mathbf{p_r}\cdot\mathbf{r}+\sum_i z_i(\grave{q}_{z,i}+\acute{q}_{z,i})=p_r r+\tau. \quad (3)$$

Formulas (1)–(3) for the τ-p transform remain valid regardless of the type of anisotropy and the type of waves (i.e., P, SV, SH).

In order to calculate traveltime curves in layered anisotropic media using equation (3), we need a mathematical description of the $\tau(\mathbf{p_r})$ curves. For the downgoing waves, such an expression can be derived using the fact that the one-way interval zero-offset traveltime, $\Delta\grave{t}_{0,i}$, equals the interval intercept time of the vertically downgoing wave, $\Delta\grave{\tau}_{0,i}$. That is, $\Delta\grave{\tau}_{0,i}=\Delta\grave{t}_{0,i}=z_i/\grave{v}_{0,i}$ with $\grave{v}_{0,i}$ the phase velocity of the vertically downgoing wave. Hence,

$$\Delta\grave{\tau}_i/\Delta\grave{\tau}_{0,i}=\frac{z_i\grave{q}_{z,i}}{z_i/\grave{v}_{0,i}}=\grave{v}_{0,i}\grave{q}_{z,i}=\grave{v}_{0,i}\left[\grave{v}_{ph,i}^{-2}-p_r^2\right]^{1/2}, \quad (4)$$

with $\grave{v}_{ph,i}$ the phase velocity in layer i. A similar expression exists for the upgoing waves. Therefore, the two-way $\tau(\mathbf{p_r})$ curves are expressed by

$$\begin{aligned}\Delta\tau_i/\Delta\tau_{0,i}&=\frac{(\Delta\grave{\tau}_i+\Delta\acute{\tau}_i)}{(\Delta\grave{\tau}_{0,i}+\Delta\acute{\tau}_{0,i})}=\frac{\grave{v}_{0,i}\acute{v}_{0,i}}{\grave{v}_{0,i}+\acute{v}_{0,i}}\left[\grave{q}_{z,i}+\acute{q}_{z,i}\right]\\&=\frac{\grave{v}_{0,i}\acute{v}_{0,i}}{\grave{v}_{0,i}+\acute{v}_{0,i}}\left[\left(\grave{v}_{ph,i}^{-2}-p_r^2\right)^{1/2}+\left(\acute{v}_{ph,i}^{-2}-p_r^2\right)^{1/2}\right], \quad (5)\end{aligned}$$

which follows from equations (2) and (4). Expression (5) can handle any type of anisotropy and all phases including converted waves. It simplifies if the phase velocity function of a pure-mode reflection is symmetric with respect to the horizontal plane, since in that case $\grave{q}_{z,i}=\acute{q}_{z,i}=q_{z,i}$. Therefore, for pure-mode waves traveling in both HTI and VTI media, it reduces to (paper I)

$$\Delta\tau_i/\Delta\tau_{0,i}=\frac{v_{0,i}}{v_{ph,i}}\left[1-p_r^2v_{ph,i}^2\right]^{1/2}. \quad (6)$$

Expressions (5) and (6) describe the form of the $\tau(\mathbf{p_r})$ curves. To calculate the required traveltimes for a given slowness, both the exact phase velocities and the emergence offset $\mathbf{r}$ are needed. These are derived in the next subsection.

Exact traveltimes and conversion points: Forward modeling

For general anisotropy and smoothly varying media, the Christoffel equation provides the phase velocities for a given plane-wave propagation direction (i.e., normal to wave front) [see, for instance, Auld (1973)]. The associated horizontal slowness $\mathbf{p_r}$ can then be obtained by dividing the horizontal component of the wavefront normal $\mathbf{n_r}$ by the phase velocity v_{ph}. That is, $\mathbf{p_r}=\mathbf{n_r}/v_{ph}$. Upon interaction with a horizontal interface, the horizontal slowness $\mathbf{p_r}$ of incident, transmitted, reflected, and converted waves has to be preserved (Snell's law). Unfortunately, solving the Christoffel equation for $\mathbf{p_r}$ results in a sixth-order polynomial equation with possibly complex roots—a common problem while ray tracing in anisotropic structures (Gajewski and Pšenčík, 1987; Kendall and Thomson, 1989). We have to deal with a similar problem to compute the desired $\tau(\mathbf{p_r})$ curves.

On the other hand, for VTI, HTI, unrotated orthorhombic, and even unrotated monoclinic media, exact expressions for the phase velocities are known (Fryer and Frazer, 1987; Tsvankin, 1996, 1997a, b). In addition, these formulas can be expressed in terms of Thomsen's (1986) parameters or generalizations thereof (Mensch and Rasolofosaon, 1997; Tsvankin, 1997a; Pšenčík and Gajewski, 1998) and finally be reordered such that they yield the exact phase velocity as a function of the horizontal slowness. Therefore, the desired $\tau(\mathbf{p_r})$ curves can be computed analytically, thereby circumventing the problem of solving sixth-order polynomial expressions.

In HTI media, the common notation of SH and SV waves is not appropriate. We therefore change to the notation of Tsvankin (1997b). If we imagine that VTI symmetry is caused by fine-scale layering (isotropic horizontal layers) and HTI symmetry by parallel vertical cracks, then the symmetry axis is perpendicular to the layering and the crack planes, respectively. The S-phases polarized parallel to the layering are called $S_\parallel$ (previously SH) and the S-waves polarized within any plane containing the symmetry axis $S_\perp$ (previously SV) since they are perpendicular to the layering [see Figure 1 in Tsvankin (1997b)]. Note that Crampin (1981) uses a similar definition. In his notation, SP corresponds to $S_\perp$ (SV) and SR to $S_\parallel$ (SH). The last two notations are unambiguous for both HTI and VTI symmetries. We will henceforth employ Tsvankin's notation in terms of P, $S_\parallel$, and $S_\perp$.

In this new notation, phase velocities of respectively P- and $S_\perp$-waves in the crystallographic coordinate system of transversely isotropic media with a vertical symmetry axis are described by (Thomsen, 1986; Tsvankin, 1996)

$$v_P^{(T)}(\theta)=\alpha_0^{(T)}\left[1+\varepsilon^{(T)}\sin^2\theta-\frac{1}{2}f^{(T)}\left(1-\sqrt{s_\theta^{(T)}}\right)\right]^{1/2}, \quad (7)$$

$$v_{S_\perp}^{(T)}(\theta)=\alpha_0^{(T)}\left[1+\varepsilon^{(T)}\sin^2\theta-\frac{1}{2}f^{(T)}\left(1+\sqrt{s_\theta^{(T)}}\right)\right]^{1/2}, \quad (8)$$

with

$$s_\theta^{(T)} = 1 + \frac{4\sin^2\theta}{f^{(T)}}\left(2\delta^{(T)}\cos^2\theta - \varepsilon^{(T)}\cos(2\theta)\right) + \frac{4\left[\varepsilon^{(T)}\right]^2\sin^4\theta}{\left[f^{(T)}\right]^2}, \tag{9}$$

and

$$f^{(T)} = 1 - \left[\beta_0^{(T)}/\alpha_0^{(T)}\right]^2. \tag{10}$$

The phase angle θ represents the polar angle with the vertical axis. The quantities $\alpha_0^{(T)}$, $\beta_0^{(T)}$, $\delta^{(T)}$, and $\varepsilon^{(T)}$ are the so-called generic Thomsen parameters with $\alpha_0^{(T)}$ and $\beta_0^{(T)}$ the phase velocities along the symmetry axis. The definitions of $\delta^{(T)}$ and $\varepsilon^{(T)}$ are given in Thomsen (1986). The generic Thomsen parameters are defined in the so-called crystallographic coordinate system, which is independent of the global coordinate system (i.e., with respect to the earth's surface). The appropriate expressions for $S_\parallel$ (SH) are contained in the Appendix.

VTI media.—For unrotated media, the crystallographic and the global coordinate systems are coincident. Therefore, the phase velocities in a VTI medium are also computed using $v_P^{(T)}(\theta)$ and $v_{S_\perp}^{(T)}(\theta)$, expressions (7) and (8). To distinguish these parameters from an HTI medium, we use the superscript $^{(\mathbf{v})}$. That is,

$$\begin{aligned} &\alpha_0^{(\mathbf{v})} = \alpha_0^{(T)}, \quad \beta_0^{(\mathbf{v})} = \beta_0^{(T)}, \\ &\delta^{(\mathbf{v})} = \delta^{(T)}, \qquad\qquad \ldots \text{VTI} \\ &\varepsilon^{(\mathbf{v})} = \varepsilon^{(T)}, \quad f^{(\mathbf{v})} = f^{(T)}. \end{aligned} \tag{11}$$

Using Snell's law,

$$p_r = \sin(\theta)/v_{ph}, \tag{12}$$

and reordering terms yields the required expressions for the phase velocity expressed as a function of the horizontal slowness. Hence,

$$v_P^{(\mathbf{v})}(p_r) = \alpha_0^{(\mathbf{v})} \times \left[\frac{2 - f^{(\mathbf{v})} + 2\left(\delta^{(\mathbf{v})}f^{(\mathbf{v})} - \varepsilon^{(\mathbf{v})}\right)\left[w_{\alpha_0}^{(\mathbf{v})}\right]^2 + f^{(\mathbf{v})}\sqrt{s_p^{(\mathbf{v})}}}{2 - 4\varepsilon^{(\mathbf{v})}\left[w_{\alpha_0}^{(\mathbf{v})}\right]^2 - 4f^{(\mathbf{v})}\left(\varepsilon^{(\mathbf{v})} - \delta^{(\mathbf{v})}\right)\left[w_{\alpha_0}^{(\mathbf{v})}\right]^4}\right]^{1/2} \tag{13}$$

for P-waves, and

$$v_{S_\perp}^{(\mathbf{v})}(p_r) = \alpha_0^{(\mathbf{v})} \times \left[\frac{2 - f^{(\mathbf{v})} + 2\left(\delta^{(\mathbf{v})}f^{(\mathbf{v})} - \varepsilon^{(\mathbf{v})}\right)\left[w_{\alpha_0}^{(\mathbf{v})}\right]^2 - f^{(\mathbf{v})}\sqrt{s_p^{(\mathbf{v})}}}{2 - 4\varepsilon^{(\mathbf{v})}\left[w_{\alpha_0}^{(\mathbf{v})}\right]^2 - 4f^{(\mathbf{v})}\left(\varepsilon^{(\mathbf{v})} - \delta^{(\mathbf{v})}\right)\left[w_{\alpha_0}^{(\mathbf{v})}\right]^4}\right]^{1/2} \tag{14}$$

for $S_\perp$-waves (paper I). In both expressions,

$$s_p^{(\mathbf{v})} = 1 + 4\left(\frac{2\delta^{(\mathbf{v})} - \varepsilon^{(\mathbf{v})}}{f^{(\mathbf{v})}} - \delta^{(\mathbf{v})}\right)\left[w_{\alpha_0}^{(\mathbf{v})}\right]^2 + 8 \times \left(\frac{1}{2}\left[\delta^{(\mathbf{v})}\right]^2 + \delta^{(\mathbf{v})} - \varepsilon^{(\mathbf{v})} + \frac{\varepsilon^{(\mathbf{v})} - \delta^{(\mathbf{v})} - \delta^{(\mathbf{v})}\varepsilon^{(\mathbf{v})}}{f^{(\mathbf{v})}} + \frac{\left[\varepsilon^{(\mathbf{v})}\right]^2}{2\left[f^{(\mathbf{v})}\right]^2}\right)\left[w_{\alpha_0}^{(\mathbf{v})}\right]^4, \tag{15}$$

and

$$w_{\alpha_0}^{(\mathbf{v})} = \alpha_0^{(\mathbf{v})}p_r. \tag{16}$$

It should be noted that, since a VTI medium is symmetric with respect to the vertical axis, the phase velocities only depend on the absolute horizontal slowness p_r and not on azimuth. Equation (A-2) yields $v_{S_\parallel}^{(\mathbf{v})}(p_r)$, the phase velocity for $S_\parallel$-waves.

HTI media.—In case of an HTI medium, however, the crystallographic symmetry axis is tilted by 90°. Hence, the crystallographic and medium coordinate system are no longer coincident. Nonetheless, in the vertical plane which now contains the horizontal symmetry axis, wave propagation phenomena can still be described using an "equivalent" VTI medium [see Tsvankin (1997b) and his Figure 2]. Therefore, within this symmetry plane, phase velocities are described by

$$v_P^{(\mathbf{h})}(\bar\theta) = \alpha_0^{(\mathbf{h})}\left[1 + \varepsilon^{(\mathbf{h})}\sin^2\bar\theta - \frac{1}{2}f^{(\mathbf{h})}\left(1 - \sqrt{s_{\bar\theta}^{(\mathbf{h})}}\right)\right]^{1/2}, \tag{17}$$

$$v_{S_\perp}^{(\mathbf{h})}(\bar\theta) = \alpha_0^{(\mathbf{h})}\left[1 + \varepsilon^{(\mathbf{h})}\sin^2\bar\theta - \frac{1}{2}f^{(\mathbf{h})}\left(1 + \sqrt{s_{\bar\theta}^{(\mathbf{h})}}\right)\right]^{1/2}, \tag{18}$$

with

$$s_{\bar\theta}^{(\mathbf{h})} = 1 + \frac{4\sin^2\bar\theta}{f^{(\mathbf{h})}}\left(2\delta^{(\mathbf{h})}\cos^2\bar\theta - \varepsilon^{(\mathbf{h})}\cos(2\bar\theta)\right) + \frac{4[\varepsilon^{(\mathbf{h})}]^2\sin^4\bar\theta}{[f^{(\mathbf{h})}]^2}. \tag{19}$$

The phase angle $\bar\theta$ within the symmetry plane is measured from the vertical. The generic Thomsen parameters $^{(T)}$ have now been replaced by the equivalent VTI quantities given by (Tsvankin, 1997b)

$$\begin{aligned} &\alpha_0^{(\mathbf{h})} = \alpha_0^{(T)}\sqrt{1 + 2\varepsilon^{(T)}}, \qquad \beta_{0\perp}^{(\mathbf{h})} = \beta_0^{(T)}, \\ &\delta^{(\mathbf{h})} = \frac{\delta^{(T)} - 2\varepsilon^{(T)}\left[1 + \varepsilon^{(T)}/f^{(T)}\right]}{\left[1 + 2\varepsilon^{(T)}\right]\left[1 + 2\varepsilon^{(T)}/f^{(T)}\right]}, \qquad \ldots \text{HTI} \\ &\varepsilon^{(\mathbf{h})} = -\frac{\varepsilon^{(T)}}{1 + 2\varepsilon^{(T)}}, \qquad f^{(\mathbf{h})} = 1 - \left[\beta_{0\perp}^{(\mathbf{h})}/\alpha_0^{(\mathbf{h})}\right]^2. \end{aligned} \tag{20}$$

The generic Thomsen parameters $^{(T)}$ are still expressed in the crystallographic coordinate system and are therefore

quantified along the horizontal symmetry axis in the actual medium. That is, for instance $\alpha_0^{(T)}$ corresponds now to the horizontal P-wave velocity along the symmetry axis in the actual medium and not to the vertical velocity. Note that Tsvankin (1997b) uses the superscript $^{(V)}$ to denote the Thomsen parameters of the equivalent VTI medium (i.e., $\alpha_0^{(\mathbf{h})}$ is equal to $\alpha_0^{(V)}$ in his notation, which should not be confused with $\alpha_0^{(\mathbf{v})}$).

To derive more general expressions of the phase velocity for HTI media, we replace $\bar{\theta}$ with the phase angle θ' with respect to the horizontal symmetry axis ($\bar{\theta} = 90^\circ - \theta'$). Thus, all $\cos(\bar{\theta})$ terms are replaced by $\sin(\theta')$, etc. Next, we make use of the fact that the medium remains axisymmetric, albeit with respect to the horizontal symmetry axis. Hence, the resulting expressions describe the actual phase velocity for any plane-wave direction with angle θ' to the symmetry axis and are not necessarily confined to the vertical symmetry plane (Tsvankin, 1997b).

If we assume that the actual symmetry axis is oriented along the x-axis, then

$$\cos(\theta') = n_x = \sin(\theta)\cos(\phi), \tag{21}$$

with n_x the x-component of the plane wave normal, θ the polar angle, and ϕ the azimuth as measured from the x-axis. Thus, phase velocities in HTI media are computed using

$$v_P^{(\mathbf{h})}(\theta,\phi) = \alpha_0^{(\mathbf{h})} \times\left[1 + \varepsilon^{(\mathbf{h})}\sin^2\theta\cos^2\phi - \frac{1}{2}f^{(\mathbf{h})}\left(1 - \sqrt{s_\theta^{(\mathbf{h})}}\right)\right]^{1/2}, \tag{22}$$

$$v_{S_\perp}^{(\mathbf{h})}(\theta,\phi) = \alpha_0^{(\mathbf{h})} \times\left[1 + \varepsilon^{(\mathbf{h})}\sin^2\theta\cos^2\phi - \frac{1}{2}f^{(\mathbf{h})}\left(1 + \sqrt{s_\theta^{(\mathbf{h})}}\right)\right]^{1/2}, \tag{23}$$

with

$$s_\theta^{(\mathbf{h})} = 1 + \frac{4\sin^2\theta\cos^2\phi}{f^{(\mathbf{h})}}\left(2\delta^{(\mathbf{h})}(1-\sin^2\theta\cos^2\phi) - \varepsilon^{(\mathbf{h})} \times(1 - 2\sin^2\theta\cos^2\phi)\right) + \frac{4\left[\varepsilon^{(\mathbf{h})}\right]^2\sin^4\theta\cos^4\phi}{\left[f^{(\mathbf{h})}\right]^2}. \tag{24}$$

Using Snell's law, equation (12), and reordering terms again yields the desired formulas for the phase velocity as a function of the horizontal slowness. That is,

$$v_P^{(\mathbf{h})}(\mathbf{p_r}) = \alpha_0^{(\mathbf{h})} \times\left[\frac{2 - f^{(\mathbf{h})} + 2\left(\delta^{(\mathbf{h})}f^{(\mathbf{h})} - \varepsilon^{(\mathbf{h})}\right)\left[w_{\alpha_0}^{(\mathbf{h})}\right]^2 + f^{(\mathbf{h})}\sqrt{s_p^{(\mathbf{h})}}}{2 - 4\varepsilon^{(\mathbf{h})}\left[w_{\alpha_0}^{(\mathbf{h})}\right]^2 - 4f^{(\mathbf{h})}\left(\varepsilon^{(\mathbf{h})} - \delta^{(\mathbf{h})}\right)\left[w_{\alpha_0}^{(\mathbf{h})}\right]^4}\right]^{1/2} \tag{25}$$

for P-waves, and

$$v_{S_\perp}^{(\mathbf{h})}(\mathbf{p_r}) = \alpha_0^{(\mathbf{h})} \times\left[\frac{2 - f^{(\mathbf{h})} + 2\left(\delta^{(\mathbf{h})}f^{(\mathbf{h})} - \varepsilon^{(\mathbf{h})}\right)\left[w_{\alpha_0}^{(\mathbf{h})}\right]^2 - f^{(\mathbf{h})}\sqrt{s_p^{(\mathbf{h})}}}{2 - 4\varepsilon^{(\mathbf{h})}\left[w_{\alpha_0}^{(\mathbf{h})}\right]^2 - 4f^{(\mathbf{h})}\left(\varepsilon^{(\mathbf{h})} - \delta^{(\mathbf{h})}\right)\left[w_{\alpha_0}^{(\mathbf{h})}\right]^4}\right]^{1/2} \tag{26}$$

for $S_\perp$-waves. In both expressions,

$$s_p^{(\mathbf{h})} = 1 + 4\left(\frac{2\delta^{(\mathbf{h})} - \varepsilon^{(\mathbf{h})}}{f^{(\mathbf{h})}} - \delta^{(\mathbf{h})}\right)\left[w_{\alpha_0}^{(\mathbf{h})}\right]^2 + 8 \times\left(\frac{1}{2}\left[\delta^{(\mathbf{h})}\right]^2 + \delta^{(\mathbf{h})} - \varepsilon^{(\mathbf{h})} + \frac{\varepsilon^{(\mathbf{h})} - \delta^{(\mathbf{h})} - \delta^{(\mathbf{h})}\varepsilon^{(\mathbf{h})}}{f^{(\mathbf{h})}} + \frac{\left[\varepsilon^{(\mathbf{h})}\right]^2}{2\left[f^{(\mathbf{h})}\right]^2}\right)\left[w_{\alpha_0}^{(\mathbf{h})}\right]^4, \tag{27}$$

and

$$w_{\alpha_0}^{(\mathbf{h})} = \alpha_0^{(\mathbf{h})}p_r\cos(\phi). \tag{28}$$

The associated equations for the phase velocity $v_{S_\parallel}^{(\mathbf{h})}(\mathbf{p_r})$ are given by equations (A-5) and (A-6).

Formulas (25)–(27) for $v_P^{(\mathbf{h})}(\mathbf{p_r})$ and $v_{S_\perp}^{(\mathbf{h})}(\mathbf{p_r})$ are nearly identical to the corresponding expressions for $v_P^{(\mathbf{v})}(p_r)$ and $v_{S_\perp}^{(\mathbf{v})}(p_r)$ for VTI media [equations (13)–(15)], except that in the HTI case the Thomsen parameters have been replaced by equivalent VTI parameters $^{(\mathbf{h})}$ instead of the generic parameters $^{(T)}$. In addition, phase velocities in HTI media depend on azimuth, hence the difference in $w_{\alpha_0}^{(\mathbf{v})}$ and $w_{\alpha_0}^{(\mathbf{h})}$ [expressions (16) and (28)].

Moreover, for $\phi = 90^\circ$, expressions (25)– (28) for $v_P^{(\mathbf{h})}(\mathbf{p_r})$ and $v_{S_\perp}^{(\mathbf{h})}(\mathbf{p_r})$ simplify considerably, since wave propagation occurs in a so-called acoustic or isotropy plane. In this case, the velocities reduce to $\alpha_0^{(T)}(1+2\varepsilon^{(T)})^{1/2}$ and $\beta_0^{(T)}$ for P and $S_\perp$-waves, respectively, and reflection moveout of pure-mode phases becomes perfectly hyperbolic.

For general HTI media, the symmetry axes of the individual layers i are rarely all oriented along the x-axis, but along an azimuth $\phi_{0,i}$. Therefore, expression (28) has to be replaced by

$$w_{\alpha_0}^{(\mathbf{h})} = \alpha_{0,i}^{(\mathbf{h})}p_r\cos(\phi - \phi_{0,i}). \tag{29}$$

Traveltimes.—Using the above expressions for the phase velocity, a very simple procedure produces the exact moveout curves in the time domain (see also paper I). Namely, for a given slowness $\mathbf{p_r}$, the $\tau(\mathbf{p_r})$ expressions (3) and (5) for converted waves or expressions (3) and (6) for pure-mode data produce the exact intercept time $\tau(\mathbf{p_r})$ in both HTI and VTI media. The required phase velocities for both P- and $S_\perp$-waves can be computed using the expressions for $v_P^{(\mathbf{v})}(p_r)$ and $v_{S_\perp}^{(\mathbf{v})}(p_r)$ [equations (13)–(16)] for VTI media or $v_P^{(\mathbf{h})}(\mathbf{p_r})$ and $v_{S_\perp}^{(\mathbf{h})}(\mathbf{p_r})$ [equations (25)–(29)] for HTI media. The associated offset $\mathbf{r}$ is then obtained using $\mathbf{r} = -d\tau/d\mathbf{p_r}$, which can be calculated by means of a central differentiation. That is, the emergence offset $\mathbf{r}$ equals the negative local slope of the total $\tau(\mathbf{p_r})$ curves (Diebold and Stoffa, 1981).

Since VTI media are axially symmetric around the z-axis, the phase velocities do not depend on azimuth. Thus, the propagation normals of the plane waves, the emergence offsets, and the reflection/conversion points of both pure-mode and converted phases all lie in the same incidence plane (for constant azimuth). That is, the incident and reflected/converted group- and phase-velocity vectors are all confined to the sagittal plane. As a consequence, for pure VTI media, the slope of the $\tau(\mathbf{p_r})$ curves can be computed by simultaneously tracking two plane waves with slightly perturbed initial radial slownesses p_r but constant azimuth centered around a third reference wave.

Unfortunately, for HTI media, phase velocities depend on azimuth ϕ and the orientation $\phi_{0,i}$ of the symmetry axes. Hence, even for pure-mode data and perfect alignment of all symmetry axes (ϕ_0 constant), the incident and reflected group- and phase-velocity vectors are generally not confined to the same sagittal plane (unless wave propagation occurs in a symmetry plane). Either the incident and reflected group- or phase-velocity vectors can be contained in a single radial (vertical) plane. That is, for constant azimuthal ray angle, the rays (group-velocity vectors) are contained in the sagittal plane, whereas the associated plane-wave normals (phase-velocity vectors) diverge from it, and vice versa.

For converted waves, however, only the incident and converted phase-velocity vectors are still confined to a radial plane, since the radial slowness $\mathbf{p_r}$ is conserved from layer to layer (Snell's law). This remains true for randomly varying orientations $\phi_{0,i}$. As a consequence, the actual conversion points and emergence offsets of a converted wave do not necessarily lie in a radial plane in HTI-media. Therefore, estimation of common-conversion-point gathers becomes truly a 3-D problem. This will be illustrated in Figure 8 of the numerical examples.

Furthermore, the local slope of the $\tau(\mathbf{p_r})$ curves has to be computed by simultaneously tracking three plane waves with slightly perturbed initial azimuthal and radial slownesses $\mathbf{p_r}$ centered around a fourth reference wave. For sufficiently small perturbations, the $\tau(\mathbf{p_r})$ points of the three outer plane waves span a surface which is locally plane. The required derivatives with respect to p_x and p_y, and thereby the emergence offset $\mathbf{r}$, are derived from the equation of that plane.

Nonetheless, exact moveout curves and conversion points can be obtained for HTI and VTI anisotropy without the need of any Taylor-series expansions or ray tracing in the space-time domain.

Conversion points.—The exact conversion point $\mathbf{r}_{\rm ccp} = (x_{\rm ccp}, y_{\rm ccp}, 0)$ for any converted wave can be calculated in two ways. For general anisotropy models, the conversion point corresponding to a P-$S_\perp$ or P-$S_\parallel$ converted wave with slowness $\mathbf{p_r}$ that arrives at offset $\mathbf{r}$ is obtained by combining the computed $\grave{v}_{ph}(\mathbf{p_r})$ and equation (4), and then calculating again the local slope of the $\grave{\tau}(\mathbf{p_r})$ curve at that particular slowness. That is,

$$\mathbf{r}_{\rm ccp} = -d\grave{\tau}/d\mathbf{p_r} \qquad \text{with} \qquad \grave{\tau} = \sum_i \Delta\grave{\tau}_i. \tag{30}$$

The associated emergence offset $\mathbf{r}$ is computed in the usual manner.

Alternatively, for both HTI and VTI media, a much simpler method can be used. Namely, the conversion point occurs underneath the common midpoint (i.e., at half the emergence offset) of a pure-mode P-wave reflection with identical horizontal slowness $\mathbf{p_r}$ since the downgoing branches of the P-P, P-$S_\parallel$, and P-$S_\perp$ reflections for identical $\mathbf{p_r}$ are coincident (Figure 3). Thus, it simply results as a byproduct of the calculation of the P-wave reflection moveout curves. Therefore, again, no Taylor-series expansions are needed, as for instance in Thomsen (1999).

By combining the conversion points $\mathbf{r}_{\rm ccp}$ and the computed emergence offset $\mathbf{r}$ and traveltime t of the converted wave, it is possible to devise an offset-time dependent binning scheme to create common-conversion-point gathers from the initial common-source gathers. Such schemes can naturally be devised for both three-component data (e.g., ocean-bottom cables) and full nine-component data.

Approximate traveltimes and conversion points: Parameter estimation

The τ-p transform can also be used for inversion purposes to estimate the anisotropy parameters in a region using equations (3) and (5) or (6) which describe the form of the $\tau(\mathbf{p_r})$ curves. However, a strong nonuniqueness exists. That is, a range of HTI and VTI models exists with identical moveout curves but different anisotropy parameters. Hence, a reduction of the total number of parameters is needed to increase the uniqueness of the inversion results (paper I). Unfortunately, different number of parameters are required for VTI or HTI symmetries due to the azimuthally dependent traveltimes in the latter case.

VTI media.—For VTI media and pure-mode P-wave data, it is possible to accurately express the $\tau(p_r)$ curves in terms of the P-wave stack velocity $\alpha_n^{(\mathbf{v})}$ and the anisotropy parameter $\eta^{(\mathbf{v})}$ only using the acoustic approximation for the vertical slowness of Alkhalifah (1998) (see paper I). Namely,

$$\tau^2(p_r)/\tau_0^2 \approx 1 - \frac{\left[w_{\alpha n}^{(\mathbf{v})}\right]^2}{1 - 2\eta^{(\mathbf{v})}\left[w_{\alpha n}^{(\mathbf{v})}\right]^2} \tag{31}$$

with

$$w_{\alpha n}^{(\mathbf{v})} = \alpha_n^{(\mathbf{v})} p_r. \tag{32}$$

The P-wave normal-moveout (NMO) velocity $\alpha_n^{(\mathbf{v})}$ and the anisotropy parameter $\eta^{(\mathbf{v})}$ are defined as (Thomsen, 1986; Alkhalifah and Tsvankin, 1995)

$$\begin{aligned} \alpha_n^{(\mathbf{v})} &= \alpha_0^{(\mathbf{v})}\left(1 + 2\delta^{(\mathbf{v})}\right)^{1/2}, \\ \eta^{(\mathbf{v})} &= \left(\varepsilon^{(\mathbf{v})} - \delta^{(\mathbf{v})}\right) / \left(1 + 2\delta^{(\mathbf{v})}\right). \end{aligned} \tag{33}$$

However, for converted wave data, we require an explicit formula for the P-wave phase velocity. Such a relation can be derived by expressing $\alpha_0^{(\mathbf{v})}$ and $\varepsilon^{(\mathbf{v})}$ in terms of the P-wave stack velocity $\alpha_n^{(\mathbf{v})}$ and the anisotropy parameter $\eta^{(\mathbf{v})}$, and by neglecting all remaining terms containing $\delta^{(\mathbf{v})}$. The resulting equation can be simplified even further by applying again an acoustic approximation ($\beta_0^{(\mathbf{v})} = 0$), yielding

$$\tilde{v}_{P,\eta}^{(\mathbf{v})}(p_r) \approx \alpha_n^{(\mathbf{v})}\left[\frac{1 - 2\eta^{(\mathbf{v})}\left[w_{\alpha n}^{(\mathbf{v})}\right]^2}{1 - 2\eta^{(\mathbf{v})}\left[w_{\alpha n}^{(\mathbf{v})}\right]^2 - 2\eta^{(\mathbf{v})}\left[w_{\alpha n}^{(\mathbf{v})}\right]^4}\right]^{1/2}. \tag{34}$$

In this expression, the influence of $\delta^{(\mathbf{v})}$ is assumed to be primarily expressed by $\eta^{(\mathbf{v})}$. Furthermore, it should be noted that $\tilde{v}^{(\mathbf{v})}_{P,\eta}(p_r)$ does not constitute a good approximation to $v^{(\mathbf{v})}_P(p_r)$, equation (13), unless used in combination with expressions (5) or (6) for the $\tau(p_r)$ curves, and $v_{0,i} = \alpha^{(\mathbf{v})}_{n,i}$. However, for pure-mode P-wave data, expressions (34) and (6) still yield the two-parameter expression (31) for the $\tau(p_r)$ curves which was derived in a completely different way using the acoustic approximation for the vertical P-wave slowness of Alkhalifah (1998).

For $S_\perp$-waves, the phase velocity function $v^{(\mathbf{v})}_{S_\perp}(p_r)$, relations (14)–(16), can respectively be replaced by (paper I)

$$\tilde{v}^{(\mathbf{v})}_{S_\perp,\sigma}(p_r) \approx \beta^{(\mathbf{v})}_0 \left[\frac{-1 + 2\sigma^{(\mathbf{v})}\left[w^{(\mathbf{v})}_{\beta_0}\right]^2 + \left\{\left(1 - 2\sigma^{(\mathbf{v})}\left[w^{(\mathbf{v})}_{\beta_0}\right]^2\right)^2 + 8\sigma^{(\mathbf{v})}\left[w^{(\mathbf{v})}_{\beta_0}\right]^4\right\}^{1/2}}{4\sigma^{(\mathbf{v})}\left[w^{(\mathbf{v})}_{\beta_0}\right]^4} \right]^{1/2}, \tag{35}$$

$$w^{(\mathbf{v})}_{\beta_0} = \beta^{(\mathbf{v})}_0 p_r, \tag{36}$$

$$\sigma^{(\mathbf{v})} = \left(\varepsilon^{(\mathbf{v})} - \delta^{(\mathbf{v})}\right)\left[\alpha^{(\mathbf{v})}_0/\beta^{(\mathbf{v})}_0\right]^2, \tag{37}$$

if we assume that first-order approximations are sufficiently accurate for $S_\perp$-waves. Note that if the denominator in equation (35) approaches zero, $\tilde{v}^{(\mathbf{v})}_{S_\perp,\sigma}$ converges to $\beta^{(\mathbf{v})}_0$. Furthermore, $v_{0,i} = \beta^{(\mathbf{v})}_{0,i}$ in expressions (5) and (6).

Moreover, from the definition of the anisotropy parameters $\eta^{(\mathbf{v})}$ and $\sigma^{(\mathbf{v})}$, equations (33) and (37), it follows that $\sigma^{(\mathbf{v})} = \eta^{(\mathbf{v})}[\alpha^{(\mathbf{v})}_n/\beta^{(\mathbf{v})}_0]^2$. Hence, in VTI media, two-parameter expressions hold for pure-mode data (i.e., $\alpha^{(\mathbf{v})}_n$ and $\eta^{(\mathbf{v})}$ for P-waves, and $\beta^{(\mathbf{v})}_0$ and $\sigma^{(\mathbf{v})}$ for $S_\perp$-waves) and three-parameter expressions for P–$S_\perp$ converted waves (i.e., $\alpha^{(\mathbf{v})}_n$, $\beta^{(\mathbf{v})}_0$, and $\eta^{(\mathbf{v})}$). It is also possible to rewrite expression (35) for the $S_\perp$-phase velocity $\tilde{v}^{(\mathbf{v})}_{S_\perp,\sigma}(p_r)$ in terms of the $S_\perp$-wave stacking velocity $\beta^{(\mathbf{v})}_{n\perp}$ using $\beta^{(\mathbf{v})}_{n\perp} = \beta^{(\mathbf{v})}_0(1 + 2\sigma^{(\mathbf{v})})^{1/2}$. However, $v_{0,i}$ remains equal to $\beta^{(\mathbf{v})}_{0,i}$ in that case.

Reflection moveout of $S_\parallel$-waves in VTI media is perfectly described using a constant velocity [expression (A-3) in the Appendix]. Table 1 summarizes the anisotropy parameters affecting moveout in VTI media.

Table 1. Necessary parameters used in the inverse problem to estimate anisotropy.*

Phase	VTI	HTI
P-P	$\alpha^{(\mathbf{v})}_n$, $\eta^{(\mathbf{v})}$	$\alpha^{(\mathbf{h})}_0$, $\delta^{(\mathbf{h})}$, $\varepsilon^{(\mathbf{h})}$, ϕ_0
$S_\perp$-$S_\perp$	$\beta^{(\mathbf{v})}_0$, $\sigma^{(\mathbf{v})}$	$\beta^{(\mathbf{h})}_{0\perp}$, $\sigma^{(\mathbf{h})}$, ϕ_0
$S_\parallel$-$S_\parallel$	$\beta^{(\mathbf{v})}_{n\parallel}$	$\beta^{(\mathbf{h})}_{0\parallel}$, $\gamma^{(\mathbf{h})}$, ϕ_0
P-$S_\perp$	$\alpha^{(\mathbf{v})}_n$, $\beta^{(\mathbf{v})}_0$, $\eta^{(\mathbf{v})}$	$\alpha^{(\mathbf{h})}_0$, $\beta^{(\mathbf{h})}_{0\perp}$, $\delta^{(\mathbf{h})}$, $\varepsilon^{(\mathbf{h})}$, ϕ_0
P-$S_\parallel$	$\alpha^{(\mathbf{v})}_n$, $\beta^{(\mathbf{v})}_{n\parallel}$, $\eta^{(\mathbf{v})}$	$\alpha^{(\mathbf{h})}_0$, $\beta^{(\mathbf{h})}_{0\parallel}$, $\delta^{(\mathbf{h})}$, $\varepsilon^{(\mathbf{h})}$, $\gamma^{(\mathbf{h})}$, ϕ_0
$S_\perp$-$S_\parallel$	$\beta^{(\mathbf{v})}_0$, $\sigma^{(\mathbf{v})}$, $\gamma^{(\mathbf{v})}$	$\beta^{(T)}_0$, $\sigma^{(\mathbf{h})}$, $\gamma^{(T)}$, ϕ_0

*Note that for laterally homogeneous VTI media the amplitude of P-$S_\parallel$ and $S_\perp$-$S_\parallel$ reflections should be zero. Only four parameters are needed for $S_\perp$-$S_\parallel$ wave propagation in HTI media if the generic Thomsen parameters $\beta^{(T)}_0$ and $\gamma^{(T)}$ are used [relations (20) and (A-4)].

HTI media.—Unfortunately, in HTI media, phase velocities do depend on azimuth. Therefore, more parameters are needed to accurately describe wave propagation phenomena.

To obtain an idea of the minimum number of parameters required for P-wave data, we need to consider that P-wave NMO velocities in horizontal HTI media show an elliptical variation with azimuth (Tsvankin, 1997b). Hence, three variables are necessary to describe this dependence, namely two NMO velocities and the orientation of a symmetry axis. These parameters could correspond, for instance, to the stack velocity $\alpha^{(\mathbf{h})}_0$ in the isotropy plane, the (short-spread) NMO velocity $\alpha^{(\mathbf{h})}_n$ in the vertical plane containing the symmetry axis, and the orientation of the symmetry axis ϕ_0. Furthermore, in the isotropy plane ($\phi = \phi_0 \pm 90^\circ$), moveout is purely hyperbolic. Hence, P-wave, propagation in this plane is perfectly described by using $\alpha^{(\mathbf{h})}_0$ only. On the other hand, nonhyperbolic moveout occurs in the other vertical symmetry plane ($\phi = \phi_0$). Fortunately, since we can construct an equivalent VTI medium, the P-wave moveout in this plane can be accurately computed using solely $\alpha^{(\mathbf{h})}_n$ and $\eta^{(\mathbf{h})}$. All these quantities are defined in a similar way as their VTI counterparts in relations (33).

Therefore, at least four parameters are needed to calculate P-wave traveltimes in an HTI medium, namely $\alpha^{(\mathbf{h})}_0$, $\alpha^{(\mathbf{h})}_n$, $\eta^{(\mathbf{h})}$, and ϕ_0. It is naturally possible to recast $v^{(\mathbf{h})}_P(\mathbf{p_r})$ [relations (25), (27), and (29)] in this new form. On the other hand, Tsvankin (1996) showed that the shear-wave velocity $\beta^{(T)}_0$ has only a very limited influence on the P-wave velocity. Hence, it is equally well possible to fix the ratio $\beta^{(\mathbf{h})}_{0\perp}/\alpha^{(\mathbf{h})}_0$ and thereby $f^{(\mathbf{h})}$ in these equations. This also results in a four-parameter approximation for $v^{(\mathbf{h})}_P(\mathbf{p_r})$ using, say, $f^{(\mathbf{h})} = 3/4$ or 1. In the latter case, we use again an acoustic approximation which results in

$$\tilde{v}^{(\mathbf{h})}_{P,ac}(\mathbf{p_r}) \approx \alpha^{(\mathbf{h})}_0 \times \left[\frac{2 - 6\left(\varepsilon^{(\mathbf{h})} - \delta^{(\mathbf{h})}\right)\left[w^{(\mathbf{h})}_{\alpha_0}\right]^2}{2 - 4\varepsilon^{(\mathbf{h})}\left[w^{(\mathbf{h})}_{\alpha_0}\right]^2 - 4\left(\varepsilon^{(\mathbf{h})} - \delta^{(\mathbf{h})}\right)\left[w^{(\mathbf{h})}_{\alpha_0}\right]^4} \right]^{1/2}, \tag{38}$$

with $w^{(\mathbf{h})}_{\alpha_0}$ given by expression (29). In this form, $\alpha^{(\mathbf{h})}_0$ equals the stack velocity in the isotropy plane ($\phi = \phi_0 \pm 90^\circ$), and the quantities $\delta^{(\mathbf{h})}$ and $\varepsilon^{(\mathbf{h})}$ are related to the (short-spread) NMO velocity and the horizontal velocity in the other vertical symmetry plane ($\phi = \phi_0$), respectively. Furthermore, this choice directly enables us to invert for $\alpha^{(\mathbf{h})}_0$, $\delta^{(\mathbf{h})}$, and $\varepsilon^{(\mathbf{h})}$ using P-wave moveout information only. This is not possible in the VTI case without any additional information which has to be derived in an independent way (the vertical velocity $\alpha^{(\mathbf{v})}_0$ could for instance be derived from well logs, check shots, or verticle seismic profiles). As a consequence, in HTI media, the vertical P-wave velocity $\alpha^{(\mathbf{h})}_0$ can be inverted for using surface seismics only. Hence, contrary to VTI media, time-to-depth conversion is possible in HTI media using P-wave traveltime information only.

The NMO velocities of the $S_\perp$-waves also show an elliptical dependence with azimuth. Therefore, again three parameters

are needed to describe this variation. On the other hand, the $S_\perp$-velocities within the isotropy plane and along the symmetry axis are identical. Thus, in a first-order approximation, only three parameters are needed. The resulting equations are nearly identical to $\tilde{v}^{(\mathbf{v})}_{S_\perp,\sigma}(p_r)$ [equations (35) and (36)] except that they are expressed in terms of the equivalent VTI parameters $^{(\mathbf{h})}$. For completeness,

$$\tilde{v}^{(\mathbf{h})}_{S_\perp,\sigma}(\mathbf{p_r}) \approx \beta^{(\mathbf{h})}_{0\perp}\left[\frac{-1+2\sigma^{(\mathbf{h})}\left[w^{(\mathbf{h})}_{\beta_{0\perp}}\right]^2+\left\{\left(1-2\sigma^{(\mathbf{h})}\left[w^{(\mathbf{h})}_{\beta_{0\perp}}\right]^2\right)^2+8\sigma^{(\mathbf{h})}\left[w^{(\mathbf{h})}_{\beta_{0\perp}}\right]^4\right\}^{1/2}}{4\sigma^{(\mathbf{h})}\left[w^{(\mathbf{h})}_{\beta_{0\perp}}\right]^4}\right]^{1/2}, \tag{39}$$

with

$$w^{(\mathbf{h})}_{\beta_{0\perp}} = \beta^{(\mathbf{h})}_{0\perp,i}\; p_r \cos(\phi-\phi_{0,i}). \tag{40}$$

The anisotropy parameter $\sigma^{(\mathbf{h})}$ is defined in a similar way as in expression (37). As a consequence, in a first-order approximation, pure-mode $S_\perp$-moveout is described by three parameters only, namely $\beta^{(\mathbf{h})}_{0\perp}$, $\sigma^{(\mathbf{h})}$, and $\phi_{0,i}$.

For P-$S_\perp$ waves in HTI media, unfortunately all five parameters are needed since the $S_\perp$-velocity $\beta^{(\mathbf{h})}_{0\perp}$ has a direct influence on the moveout and the ratio $\beta^{(\mathbf{h})}_{0\perp}/\alpha^{(\mathbf{h})}_0$ cannot be kept constant. Thus, its traveltimes are computed using $\alpha^{(\mathbf{h})}_0$, $\beta^{(\mathbf{h})}_{0\perp}$, $\delta^{(\mathbf{h})}$, $\varepsilon^{(\mathbf{h})}$, and $\phi_{0,i}$. Unfortunately, this means that it is impossible to reduce the number of parameters in the inversion process, and recourse has to be taken to the exact equations for the phase velocities $v^{(\mathbf{h})}_p(\mathbf{p_r})$ and $v^{(\mathbf{h})}_{S_\perp}(\mathbf{p_r})$ [relations (25)–(29)]. As a consequence, no approximate P-$S_\perp$ common conversion points exist.

No reduced-parameter expressions for $v^{(\mathbf{h})}_{S_\parallel}(\mathbf{p_r})$ can be derived either. Table 1 recapitulates the required inversion parameters for all phases.

Parameter estimation.—The new phase velocity functions $\tilde{v}^{(\mathbf{v})}_{p,\eta}(p_r)$, $\tilde{v}^{(\mathbf{v})}_{S_\perp,\sigma}(p_r)$, $\tilde{v}^{(\mathbf{h})}_{P,ac}(\mathbf{p_r})$, and $\tilde{v}^{(\mathbf{h})}_{S_\perp,\sigma}(\mathbf{p_r})$ [relations (34), (35), (38), and (39)] can be used to calculate approximate traveltime curves of pure-mode data in both HTI and VTI media in a similar way as before. In addition, they can be used for inversion purposes (paper I). For P-$S_\perp$ converted waves and their conversion points, reduced-parameter expressions for the associated phase velocities can only be derived for VTI media. For HTI symmetries, the exact formulas for $v^{(\mathbf{h})}_P(\mathbf{p_r})$ and $v^{(\mathbf{h})}_{S_\perp}(\mathbf{p_r})$, equations (25)–(29), are necessary due to the azimuthal dependence of both the P and $S_\perp$ phase velocities.

Nonetheless, the appropriate inversion strategy is straightforward. First, the seismic data is transformed to the τ-p domain. Then, the semielliptical $\tau(\mathbf{p_r})$ curves are picked for several reflectors. Next, a so-called layer-stripping approach is applied. That is, the differential intercept times $\Delta\tau_i = \tau_i - \tau_{i-1}$ are computed for each layer and horizontal slowness $\mathbf{p_r}$ [see equation (2)]. Finally, using a local or global inversion scheme and equation (5) or (6), the observed $\Delta\tau_i(\mathbf{p_r})$ curves are fitted layer by layer to retrieve the anisotropy parameters of each layer, separately. The theoretical phase velocities in terms of the horizontal slowness are identical to those used to calculate approximate traveltimes and conversion points.

In practice, it is easier to pick the curves in the time-offset domain, to calculate the differential moveout which produces the required slowness ($\mathbf{p_r} = \partial t/\partial \mathbf{r}$), and to compute finally the associated $\tau(\mathbf{p_r})$ value using again the τ-p transform (3). Moreover, as a quality control, the $\tau(\mathbf{p_r})$ curves of the picked traveltime moveout can be overlain on the τ-p gathers of the data. Furthermore, an interactive procedure can be devised in which the picked curves are adapted in and compared with data in both domains.

A general inversion strategy

How can the above-described inversion method be best applied to a seismic data set? First of all, the appropriate inversion strategy depends on whether we are dealing with a single 2D line or a complete 3D acquisition geometry. As a quick reminder, Table 1 shows again the necessary parameters involved for all types of phases and both VTI and HTI symmetries.

2D data.—Naturally the 2D line is the simplest case where we can only consider VTI symmetry due to the lack of azimuthal information. Luckily, if the actual anisotropy symmetry is HTI (e.g., due to vertical cracks), we are still able to replace each vertical plane with an equivalent VTI medium. This follows from the form of $v^{(\mathbf{h})}_P(\theta,\phi)$ and $v^{(\mathbf{h})}_{S_\perp}(\theta,\phi)$ [relations (22)–(24)]. We are therefore not limited to specific orientations of the seismic line with respect to the actual symmetry axis (e.g., symmetry planes). Unfortunately, we do make the assumption that out-of-plane effects can be neglected (e.g., conversion points in homogeneous HTI media are not confined to radial planes through the source location). Furthermore, this also amounts to assuming that the medium is laterally homogeneous. Nonetheless, the inversion strategy is straightforward. Traveltime curves are picked, transformed to $\tau(p_r)$ curves, and fitted using the appropriate VTI equations.

Note, however, that if the medium actually displays orthorhombic or lower symmetry, conical points (i.e., point singularities) may occur in the phase-velocity sheets of both shear-waves [see, for instance, Crampin (1981) and Crampin and Yedlin (1981)]. The resulting wave behavior cannot be described assuming a VTI symmetry, and inaccuracies may arise in the inversion results. On the other hand, to the best of our knowledge, conical points have never been observed in seismic field data.

3D data.—If we have a complete 3D data volume, the appropriate inversion strategy is in principle the same, but becomes practically more involved. On the other hand, a 3D geometry is an absolute prerequisite if the actual anisotropic symmetry is to be established. Due to the increased volume of data, we recommend performing a preliminary analysis of the azimuthal variations of the NMO velocities of the considered horizons first before attacking the complete inverse problem.

Grechka et al. (1999) show that pure-mode NMO velocities generally display an elliptical azimuthal dependence, even for

arbitrary types of anisotropy. The orientation of the ellipse and the magnitude of its axes can be computed by examining a minimum of three lines through a common midpoint. For HTI symmetry, the fastest NMO velocity corresponds generally to the velocity in the isotropy plane, and conversely the slowest one is parallel to the symmetry axis [assuming that $\varepsilon^{(T)} > 0$ and thus $\varepsilon^{(\mathbf{h})} < 0$; see equation (20)]. However, in the case of VTI symmetry or isotropy, the ellipse collapses to a perfect circle.

Further a priori knowledge can be acquired by qualitatively looking for nonhyperbolic moveout. Both VTI and isotropic media do not display any azimuthal variation in the NMO velocities. However, only VTI symmetry yields nonhyperbolic moveout for P and $S_\perp$-waves if $\varepsilon^{(\mathbf{v})} \neq \delta^{(\mathbf{v})}$ (i.e., nonelliptical anisotropy). Similarly, both HTI and orthorhombic symmetry cause an NMO ellipse. However, in the former case, an isotropy plane without nonhyperbolic moveout must be present, and the nonhyperbolic moveout should be strongest along the second axis of the ellipse. On the other hand, if no isotropy plane can be detected, then we are clearly dealing with a more complicated anisotropy symmetry or strong lateral velocity variations. As a rule of thumb, vertical velocity gradients only cause noticeable nonhyperbolic moveout if the velocity doubles in magnitude within a layer (Hake, 1986; Alkhalifah, 1997).

A distinction between the influence of lateral velocity variations and anisotropy may be difficult to obtain using the present formalism. Nevertheless, indications of lateral inhomogeneity can be obtained by independently estimating the optimum anisotropy parameters at different locations. In addition, different moveout curves for positive and negative offsets at a single common midpoint location also strongly point to lateral changes (Thomsen, 1999).

Once the preliminary NMO velocity analysis has been performed and all possible a priori information acquired, an inversion strategy identical to that for a single 2D line can be applied. That is, traveltime curves are picked, converted to $\tau(\mathbf{p_r})$ curves, and inverted for anisotropy parameters using the appropriate expressions. However, to accurately transform the traveltime picks to the τ-p domain, slowness must be estimated from the 3D slope of the traveltime surfaces. Picks must be densely distributed, both with distance and azimuth, since otherwise aliasing may occur. In addition, in order to detect and invert for nonhyperbolic moveout, the ratio r/z has to be larger than 1.5 for all azimuths (Alkhalifah, 1997). This condition must also be met in the 2D case, otherwise deviations from hyperbolic moveout are too small to be measured. Furthermore, this condition must be met regardless whether Taylor-series expansions or τ-p methods are used to invert for the anisotropy parameters.

NUMERICAL EXAMPLE

As an illustration, we use a strongly anisotropic shale which displays a triplication in the $S_\perp$-moveout curve. Elasticity parameters are taken from Thomsen (1986) and shown in Table 2. Figure 4 displays the slowness and group-velocity surfaces. We consider a three-layer model composed of an uppermost isotropic layer ($\alpha = 2$ km/s, $\beta = 1$ km/s), an anisotropic shale layer, and again an underlying isotropic layer, ($\alpha = 4$ km/s, $\beta = 2$ km/s). Each layer has a thickness of 1 km. The same model was already considered in paper I, but we briefly revisit it here for illustrative reasons and complete it with the traveltime curves and conversion points of the P-$S_\perp$ phase.

Figure 5 displays the moveout curves. The solid lines are the exact moveout curves and the long-dash lines show the two-parameter τ-p approximations. The P-wave moveout curve is nearly indistinguishable from the exact curve, indicating the high accuracy of approximation (34) for $\tilde{v}^{(\mathbf{v})}_{P,\eta}$. The two-parameter approximation for $\tilde{v}^{(\mathbf{v})}_{S_\perp,\sigma}$ [relations (35) and (36)] for the $S_\perp$-waves is somewhat less accurate. Nevertheless, it is able to reproduce the cusp. The prediction of P-$S_\perp$ moveout is also nearly perfect.

Figure 5 also shows results of the popular Taylor-series approximations (short dashes) (Tsvankin and Thomsen, 1994; Alkhalifah and Tsvankin 1995; Thomsen, 1999). This method produces quite accurate results for the P-wave moveout curves. However, predictions are less accurate than those of the two-parameter τ-p method. For $S_\perp$-waves, the Taylor-series method only produces good approximations for short and intermediate offsets (i.e., up to the cusp). Its traveltime predictions for the P-$S_\perp$ converted wave are also inferior. Remarkably, the Taylor-series method cannot perfectly describe the P-$S_\perp$ traveltimes for reflections of the bottom of the first isotropic layer.

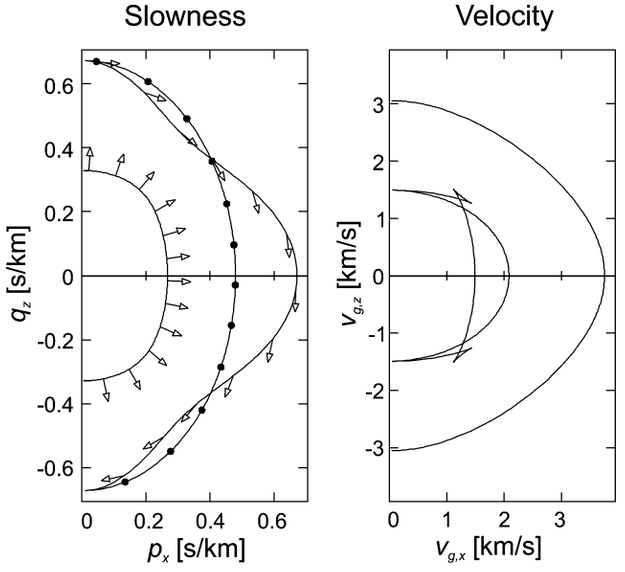

FIG. 4. Phase-slowness (left) and group-velocity (right) surfaces of the anisotropic shale described in Table 2. The velocity sheets are axisymmetric around the vertical axis.

Table 2. Elastic parameters of the shale used in the numerical examples (Figures 5–8). All values are taken from Thomsen (1986).

Generic name	$\alpha_0^{(T)}$ (km/s)	$\beta_0^{(T)}$ (km/s)	$\varepsilon^{(T)}$	$\delta^{(T)}$	$\eta^{(T)}$	$\sigma^{(T)}$	$\gamma^{(T)}$	ρ (g/cm^3)
Shale (5000)	3.048	1.490	0.255	−0.050	0.339	1.276	0.480	2.420

The moveout for $S_{\parallel}$ in VTI media is purely hyperbolic and the $\tau(p_r)$ curves elliptic. Thus, both methods predict them perfectly. Similarly, the discrepancy in the predictions for P-$S_{\parallel}$ converted waves solely depends on the accuracy of the P-wave moveout prediction. The errors are therefore comparable to those of the P-wave curves.

Figure 6 shows the exact (solid line) and approximate (long dashes) conversion points as predicted by the τ-p method. The approximations are quite accurate, with maximum errors of 100 m at 5 km offsets. In addition, the conversion point predictions of the Taylor-series method (short dashes) are shown (Thomsen, 1999). Clearly, the τ-p method produces much better results since errors of more than 1 km occur in the predictions of the Taylor-series method for the second anisotropic layer.

The results in Figures 5 and 6 do not depend on azimuth since a VTI medium is symmetric around the vertical axis. If, on the other hand, the anisotropic shale in Table 2 is tilted by 90° (HTI), this is no longer true. Figure 7 displays the exact traveltime curves of different seismic phases for reflections of the bottom of the second anisotropic layer. Traveltimes are shown for three different phase azimuths, namely along the symmetry axis (0°), at 45°, and within the isotropy plane (90°). For both P- and P-$S_{\perp}$-waves, velocities within the isotropy plane are fastest. Conversely, for $S_{\perp}$-waves at short offsets, $S_{\perp}$-velocities are slowest within this plane. On the other hand, for longer offsets, $S_{\perp}$-velocities for intermediate azimuths (45°) are fastest.

In addition, Figure 7 also displays the HTI traveltime approximations using the reduced-parameter expressions for P- and $S_{\perp}$-waves, respectively [relations (38) and (39)]. Again,

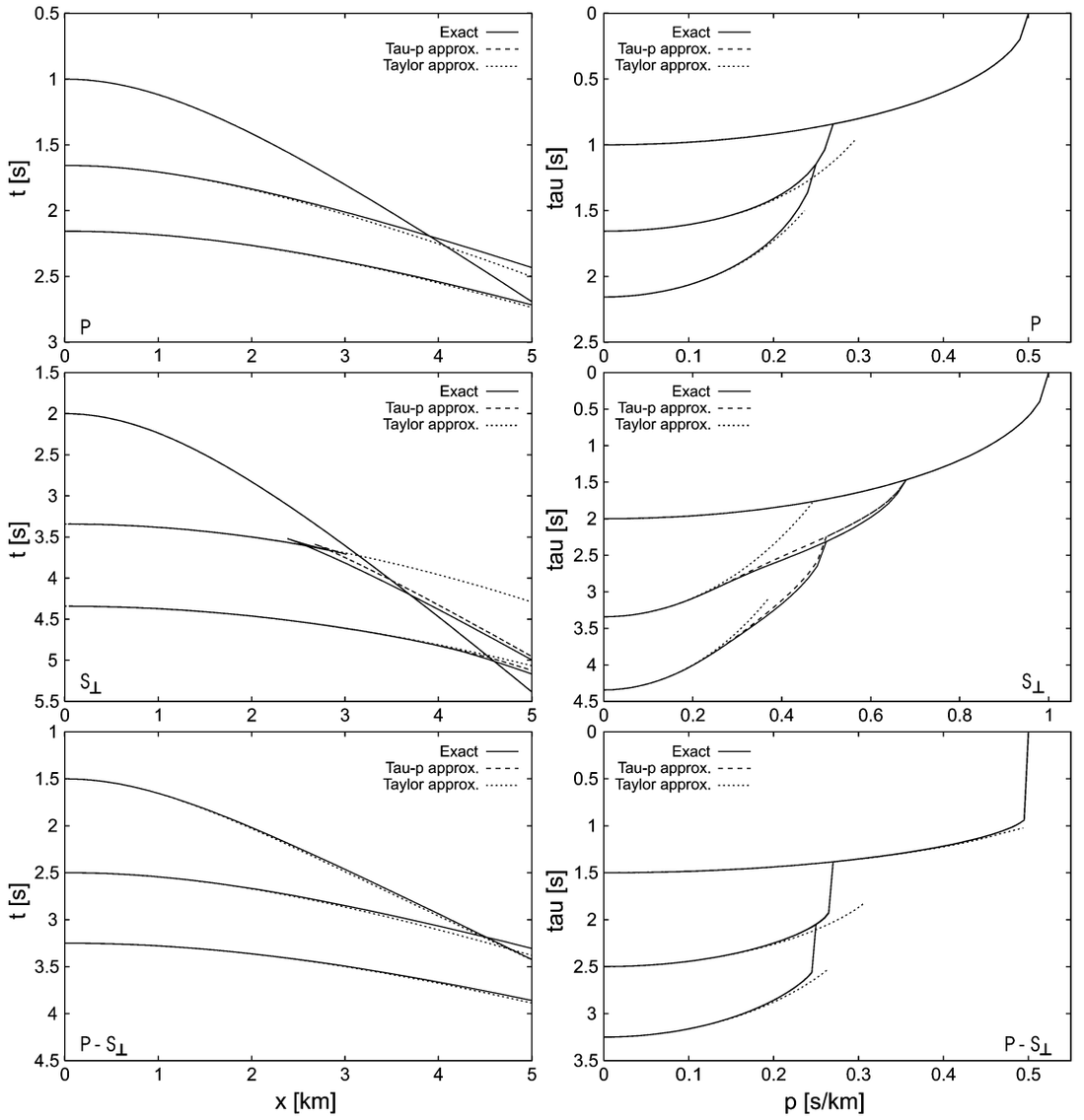

FIG. 5. Traveltimes (left) and $\tau(p_r)$ curves (right) for the three-layer VTI model for P, $S_{\perp}$, and P-$S_{\perp}$ converted waves. Note that the Taylor-series method always produces less accurate estimates than the τ-p method. Solid line: exact curves; long dashes: τ-p approximations; short dashes: Taylor-series approximations.

the results for P-waves are nearly perfect, with errors less than 5 ms at 5 km offset along the symmetry axis. The discrepancies for the $S_\perp$-waves are much larger, although predictions are again exact within the isotropy plane. The larger discrepancies at the azimuthal phase angle of 45° are partly due to the fact that the emergence positions of the exact and approximate $S_\perp$-traveltimes are increasingly divergent at larger offsets. This is due to differences in the directions of the group and phase velocities. Discrepancies are smaller at identical emergence positions. For the P-$S_\perp$ converted waves, no approximate expressions exist since all five parameters are needed in HTI media (Table 1). Traveltimes for all reflections and conversions from the bottom of the first isotropic layer are naturally exact, and the discrepancies in the predictions of the reflection moveout for the bottom of the third isotropic layer are smaller than those for the second layer.

Figure 7 also shows the Taylor-series approximations for the reflection moveout which exist for pure-mode phases only (Al-Dajani and Tsvankin, 1998). For clarity, these are only displayed for propagation along the 0° symmetry axis (short dashes). Within this symmetry plane, the τ-p approximations are clearly more accurate in the far offset, especially in the case of $S_\perp$-$S_\perp$ moveout since the Taylor-series expansions cannot handle kinks or cusps. On the other hand, for short offsets and an azimuth of 0°, the Taylor-series method is more accurate for $S_\perp$-$S_\perp$ moveout. It should be noted that errors for the Taylor-series expansions are largest within the 0° symmetry plane and reduce to zero in the isotropy plane (Al-Dajani and Tsvankin, 1998).

Finally, Figure 8 shows a plan view of the conversion points of the P-$S_\perp$ and P-$S_\parallel$ waves at the bottom of the second layer. They are displayed in two different bands with declination phase angles of respectively 60° and 75° (measured from the horizontal plane) and 11 phase angle azimuths between 0° (x-axis) and 90° (y-axis). The straight lines connect the positions of the conversion and emergence points on the surface and display therefore the horizontal projections of the upgoing shear rays. For reference, the inner circle of each band links the P-wave midpoints and the outer circle their emergence positions. The exact P-wave midpoints and conversion points for both P-$S_\perp$ and P-$S_\parallel$ waves are coincident for identical radial slownesses and azimuths (Figure 3).

For constant ray (group-velocity) azimuth, the P-wave moveout is confined to radial planes through the source location, whereas the P-$S_\perp$ converted waves display out-of-plane effects (except in the two symmetry planes). These out-of-plane conversions strongly depend on azimuth. On the other hand, the P-$S_\parallel$ moveout hardly deviates from the sagittal plane, and the approximate expressions for the P-$S_\parallel$ velocities are nearly perfect. No Taylor-series expansions exist for conversion points in HTI media and no comparison could be made.

Figure 8 clearly demonstrates that the estimation of common conversion points in HTI media is a 3D problem (offset, azimuth, traveltime) even in laterally homogeneous media. Strong variations with both offset and azimuth can occur especially for the P-$S_\perp$-waves. Hence, accurate estimation of all relevant anisotropy parameters (Table 1) becomes very important before the problem of sorting into common-conversion-point gathers can be tackled.

DISCUSSION

Our approach of computing traveltimes and conversion points in the τ-p domain makes it possible to invert for the

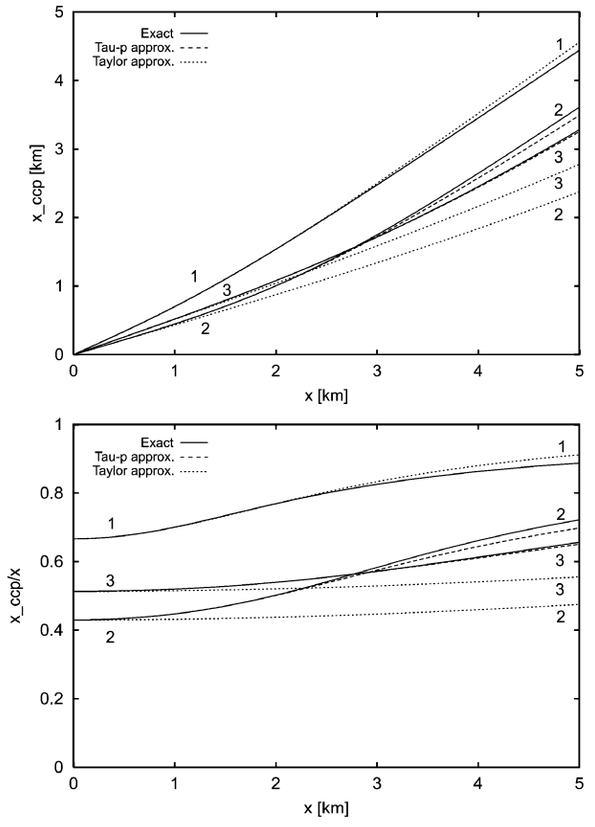

FIG. 6. Estimations of the common conversion points x_{ccp} of P-$S_\perp$ converted waves for the three-layer VTI model. Upper part: conversion point distance from the source as a function of emergence offset. Lower part: ratio x_{ccp}/x. Numbers correspond to layer indices. Solid line: exact curves; long dashes: τ-p approximations; short dashes: Taylor-series approximations.

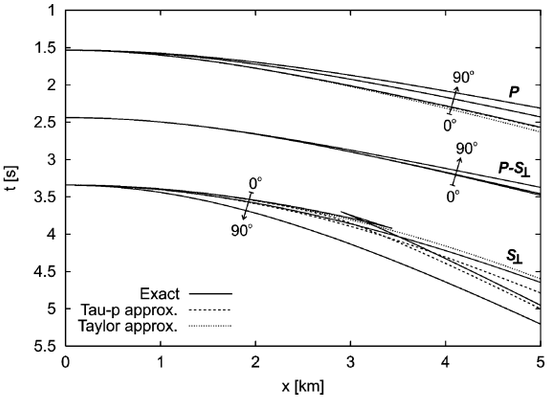

FIG. 7. Traveltimes for reflections from the bottom of the second HTI layer for P, $S_\perp$, and P-$S_\perp$ converted waves. Traveltimes are computed for constant azimuthal phase angles of 0°, 45°, and 90°. Solid line: exact curves; long dashes: τ-p approximations; short dashes: Taylor-series approximations (along symmetry axis only).

underlying anisotropy parameters in both HTI and VTI media (or combinations thereof) using a variety of seismic phases. It is suited for both offshore (streamer only or in combination with ocean-bottom cables) and onshore data (using conventional seismic or even complete nine-component data).

Furthermore, as shown in paper I, for layered, laterally homogeneous regions, a so-called layer-stripping approach is feasible. In this approach, traveltime or $\tau(\mathbf{p_r})$ curves are picked for different horizons, and the interval $\Delta\tau_i$ curves are computed to isolate the anisotropy in each individual layer. Hence, both effective (average) and local (interval) estimates are obtained. This makes the τ-p method a very powerful tool.

Moreover, Diebold (1987) showed that a similar relation between traveltime and $\tau(\mathbf{p_r})$ curves exists as expression (1) for 3D isotropic media composed of randomly dipping layers and for more general acquisition geometries other than surface seismic. However, each individual layer has to remain homogeneous. This remains true for 3D anisotropic structures. Hence, receivers and sources can be positioned at different depths, and the method can be extended to include for instance verticle-seismic-profile geometries and/or dipping layers. In addition, multiples can be included by making use of their periodicity in the τ-p domain for flat layers. Unfortunately, for randomly dipping layers, the horizontal slowness is no longer conserved, and the layer-stripping operation becomes more complicated. In addition, care has to be taken if pinch-outs are to be included. Nonetheless, both exact and approximate traveltimes and conversion points can be computed in randomly dipping HTI and VTI media. Note that the HTI and VTI symmetries are in this case defined with respect to the bottom of each layer. Furthermore, it is possible to predict reflection-point smearing for pure-mode phases (anisotropic dip moveout) and common conversion points in such structures using expression (4).

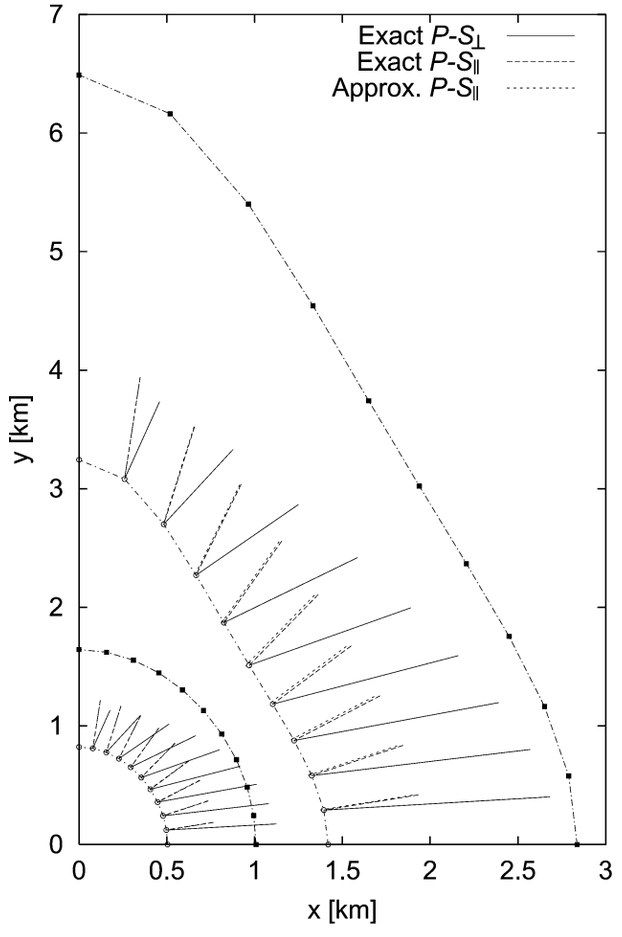

FIG. 8. Lateral distribution of conversion points of the base of the HTI layer for P-$S_\perp$ and P-$S_\parallel$ waves. Shown are the horizontal projections of the upgoing converted rays (straight lines) and the P-wave midpoints and emergence positions (symbols connected by a dot-dash line). The source is placed at the origin. Solid line: exact P-$S_\perp$ waves; long dashes: exact P-$S_\parallel$ waves; short dashes: approximate P-$S_\parallel$ waves.

Finally, expression (5) describing the form of the $\Delta\tau_i(\mathbf{p_r})$ curves remains valid for more general types of anisotropy, including tilted TI media or even lower symmetries like orthorhombic or monoclinic (with arbitrary orientation of the symmetry axes). Exact formulas for the phase velocities in the crystallographic coordinate system of such media exist (Fryer and Frazer, 1987; Tsvankin, 1996; Tsvankin, 1997a) and can be expressed in terms of Thomsen's (1986) parameters or generalizations thereof (Mensch and Rasolofosaon, 1997; Tsvankin, 1997a; Pšenčík and Gajewski, 1998). Hence, the τ-p transform is able to calculate exact traveltimes and conversion points in randomly dipping layers with arbitrary type and strength of anisotropy (although a sixth-order polynomial expression with possibly complex roots may have to be solved). In addition, expression (4) can again be used to calculate reflection-point smearing of pure-mode phases in such media and common conversion points. On the other hand, to detect the parameters most influencing the actual traveltimes and conversion points for different seismic phases and which are appropriate for inversion purposes (Table 1), further analytic treatments are warranted.

CONCLUSIONS

The τ-p approach is capable of computing exact traveltimes and conversion points for a stratified earth composed of homogeneous layers and arbitrary strength of anisotropy without the need of any ray tracing in the space-time domain. In addition to obtaining exact moveout curves and conversion points, the same method also provides approximate traveltimes and conversion points using reduced-parameter expressions for the phase velocities which are better suited for inversions. These reduced-parameter predictions yield estimates with a nearly always higher accuracy than those provided by the conventional Taylor-series expansion. Furthermore, the method has been extended in this paper to handle HTI symmetries for all azimuths and offsets.

Therefore, the τ-p approach can both be used as a forward modeling and inversion tool to assess the anisotropy parameters in a particular area. Hence, once these parameters have been determined, the associated reflection-moveout curves and common conversion points can then be computed using the same approach.

ACKNOWLEDGMENTS

M.v.d.B. thanks Shell Expro UK for financial support. We are also grateful to Tariq Alkhalifah and an anonymous reviewer

for their comments and suggestions. Tariq was again able to spot some incorrect remarks and provided us with a new reference. Finally, we thank Dirk Smit for initiating the project and for his continued interest and feedback.

REFERENCES

Al-Dajani, A., and Toksöz, N., 1999, Shear-wave reflection moveout for azimuthally anisotropic media: 69th Ann. Internat. Mtg, Soc. Expl. Geophys., Expanded Abstracts, 973–976.
Al-Dajani, A., and Tsvankin, I., 1998, Nonhyperbolic reflection moveout for horizontal transverse isotropy: Geophysics, **63**, 1738–1753.
Al-Dajani, A., Tsvankin, I., and Toksöz, M. N., 1998, Nonhyperbolic reflection moveout for azimuthally anisotropic media: 68th Ann. Internat. Mtg, Soc. Expl. Geophys., Expanded Abstracts, 1479–1482.
Alkhalifah, T., 1997, Velocity analysis using nonhyperbolic moveout in transversely isotropic media: Geophysics, **62**, 1839–1854.
———1998, Acoustic approximations for processing in transversely isotropic media: Geophysics, **63**, 623–631.
Alkhalifah, T., and Tsvankin, I., 1995, Velocity analysis for transversely isotropic media: Geophysics, **60**, 1550–1566.
Auld, B. A., 1973, Acoustic fields and waves in solids: J. Wiley and Sons.
Chapman, C. H., and Pratt, R. G., 1992, Traveltime tomography in anisotropic media—I. Theory: Geophys. J. Internat, **109**, 1–19.
Crampin, S., 1981, A review of wave motion in anisotropic and cracked elastic-media: Wave motion, **3**, 343–391.
Crampin, S., and Yedlin, M., 1981, Shear-wave singularities of wave propagation in anisotropic media: J. Geophys., **49**, 43–46.
Diebold, J. B., 1987, Three-dimensional traveltime equation for dipping layers: Geophysics, **52**, 1492–1500.
Diebold, J. B., and Stoffa, P. L., 1981, The traveltime equation, tau-p mapping, and inversion of common midpoint data: Geophysics, **46**, 238–254.
Fryer, G. J., and Frazer, L. N., 1987, Seismic waves in stratified anisotropic media—II. Elastodynamic eigensolutions for some anisotropic systems: Geophys. J. Roy. Astr. Soc., **91**, 73–101.
Gajewski, D., and Pšenčík, I., 1987, Computation of high-frequency seismic wavefields in 3-D laterally inhomogeneous anisotropic media: Geophys. J. Roy. Astr. Soc., **91**, 383–411.
Grechka, V., Tsvankin, I., and Cohen, J. K., 1999, Generalized Dix equation and analytic treatment of normal-moveout velocity for anisotropic media: Geophys. Prospect., **47**, 117–148.
Guest, W. S., and Kendall, J.-M., 1993, Modelling seismic waveforms in anisotropic inhomogeneous media using ray and Maslov asymptotic theory: Applications to exploration seismology: Can. J. Expl. Geophys., **29**, 78–92.
Hake, H., 1986, Slant stacking and its significance for anisotropy: Geophys. Prospect., **34**, 595–608.
Hudson, J. A., 1981, Wave speeds and attenuation in material containing cracks: Geophys. J. Roy. Astr. Soc., **64**, 133–150.
Kendall, J.-M., and Thomson, C. J., 1989, A comment on the form of the geometrical spreading equations, with some numerical examples of seismic ray tracing in inhomogeneous, anisotropic media: Geophys. J. Internat., **99**, 401–413.
Mensch, T., and Rasolofosaon, P., 1997, Elastic wave velocities in anisotropic media of arbitrary anisotropy—Generalization of Thomsen's parameters ϵ, δ and γ: Geophys. J. Internat., **128**, 43–64.
Pšenčík, I., and Gajewski, D., 1998, Polarization, phase velocity, and NMO velocity of qP-waves in arbitrary weakly anisotropic media: Geophysics, **63**, 1754–1766.
Thomsen, L., 1986, Weak anisotropy: Geophysics, **51**, 1954–1966.
———1999, Converted-wave reflection seismology over inhomogeneous, anisotropic media: Geophysics, **64**, 678–690.
Tsvankin, I., 1996, P-wave signatures and notation for transversely isotropic media: An overview: Geophysics, **61**, 467–483.
———1997a, Anisotropic parameters and P-wave velocity for orthorhombic media: Geophysics, **62**, 1292–1309.
———1997b, Reflection moveout and parameter estimation for horizontal transverse isotropy: Geophysics, **62**, 614–629.
Tsvankin, I., and Thomsen, L., 1994, Nonhyperbolic reflection moveout in anisotropic media: Geophysics, **59**, 1290–1304.
Van der Baan, M., and Kendall, J.-M., 2002, Estimating anisotropy parameters and traveltimes in the τ-p domain: Geophysics, **67**, 1076–1086.

APPENDIX

PHASE VELOCITY EXPRESSIONS FOR $S_\parallel$-WAVES

For completeness, the appropriate relations for $S_\parallel$ (SH) moveout are given in this Appendix. In the crystallographic coordinate system, the phase velocity of $S_\parallel$-waves is completely described by the generic Thomsen parameters $\beta_0^{(T)}$ and $\gamma^{(T)}$. That is,

$$v_{S_\parallel}^{(T)}(\theta) = \beta_0^{(T)}\left(1 + 2\gamma^{(T)}\sin^2\theta\right)^{1/2}. \tag{A-1}$$

The definition of $\gamma^{(T)}$ is given in Thomsen (1986). As for $S_\perp$-waves, $\beta_0^{(T)}$ equals the phase velocity along the symmetry axis and is identical for both S-waves.

VTI media

Since the crystallographic and global coordinate system are coincident in VTI media, the VTI parameters$^{(\mathbf{v})}$ are equal to their generic counterparts, i.e., $\gamma^{(\mathbf{v})} = \gamma^{(T)}$ and $\beta_{0\parallel}^{(\mathbf{v})} = \beta_0^{(T)}$ $(= \beta_{0\perp}^{(\mathbf{v})} = \beta_0^{(\mathbf{v})})$. Hence, equation (A-1) also provides the phase velocities in VTI media. To obtain the required velocities as a function of horizontal slowness, Snell's law (12) is substituted in expression (A-1), yielding

$$v_{S_\parallel}^{(\mathbf{v})}(p_r) = \beta_0^{(\mathbf{v})}\left(1 - 2\gamma^{(\mathbf{v})}\left[w_{\beta_0}^{(\mathbf{v})}\right]^2\right)^{-1/2}, \tag{A-2}$$

with $w_{\beta_0}^{(\mathbf{v})} = \beta_0^{(\mathbf{v})} p_r$ [equation (36)]. $S_\parallel$-moveout is always perfectly hyperbolic even for very strong anisotropy. As a consequence, it is similar to P-wave moveout in media characterized by elliptical anisotropy ($\varepsilon^{(\mathbf{v})} = \delta^{(\mathbf{v})}$) in that it can be described using a single parameter. Therefore, exact traveltimes and $\tau(p_r)$ curves are computed using a constant velocity. Namely,

$$\tilde{v}_{S_\parallel,\gamma}^{(\mathbf{v})}(p_r) = \beta_{n\parallel}^{(\mathbf{v})} = \beta_0^{(\mathbf{v})}\left(1 + 2\gamma^{(\mathbf{v})}\right)^{1/2}, \tag{A-3}$$

with $v_{0,i} = \beta_{n\parallel,i}^{(\mathbf{v})}$ in relations (5) and (6) governing the $\tau(p_r)$ curves.

HTI media

For HTI symmetry, the crystallographic and global coordinate systems are not coincident but tilted by 90°. Nevertheless, we can again replace the HTI medium with an equivalent VTI medium using (Tsvankin, 1997b)

$$\begin{aligned} \beta_{0\parallel}^{(\mathbf{h})} &= \beta_0^{(T)}\left(1 + 2\gamma^{(T)}\right)^{1/2}, \\ \gamma^{(\mathbf{h})} &= -\frac{\gamma^{(T)}}{1 + 2\gamma^{(T)}}. \end{aligned} \tag{A-4}$$

However, this equivalent VTI medium is not identical to the one employed for P-$S_\perp$ motion [expressions (20)] since two different S-wave phase velocities along the vertical axis are used ($\beta_{0\parallel}^{(\mathbf{h})} \neq \beta_{0\perp}^{(\mathbf{h})}$). Nonetheless, both replacement media can be used simultaneously.

Following a similar derivation as before, the phase velocity $v_{S_\parallel}^{(\mathbf{h})}(\mathbf{p_r})$ as a function of horizontal slowness can be derived, resulting in

$$v_{S_\parallel}^{(\mathbf{h})}(\mathbf{p_r}) = \beta_{0\parallel}^{(\mathbf{h})}\left(1 - 2\gamma^{(\mathbf{h})}\left[w_{\beta_{0\parallel}}^{(\mathbf{h})}\right]^2\right)^{-1/2}, \tag{A-5}$$

with

$$w_{\beta_{0\parallel}}^{(\mathbf{h})} = \beta_{0\parallel}^{(\mathbf{h})} p_r \cos(\phi - \phi_0). \tag{A-6}$$

For HTI symmetry, no reduced-parameter expression for $v_{S_\parallel}^{(\mathbf{h})}(\mathbf{p_r})$ can be derived due to its azimuthal dependence (Table 1).